Chapter 14
Orbit Geometry and Determination

14.1 Orbit Geometry

In this section we derive some useful formulas for the design of satellite missions.

14.1.1 Eclipse Duration

Satellites in planetary orbits are generally subject to eclipse. Because they are usually powered by solar cells, their electric power system needs to be designed such that even throughout the eclipse the satellite is sufficiently powered. It is therefore crucial to know the eclipse duration of the satellite. This is derived in the following for a circular orbit.

As it turns out, a key parameter is the so-called *beta angle* (a.k.a. *orbit beta angle*) as shown in Fig. 14.1. The beta angle is the angle between the solar vector and the orbit plane. If the solar vector lies in the orbit plane $\beta = 0°$, if it is normal to it $\beta = 90°$. Hence $0° \leq \beta \leq 90°$.

From trigonometry it can be shown that the beta angle is given by the orbital elements as

$$\sin\beta = \sin i \cdot \cos\delta_S \cdot \sin(\Omega - \Omega_S) + \cos i \cdot \sin\delta_S \tag{14.1.1}$$

with

- i Orbit inclination
- Ω Right ascension of ascending node (RAAN) of the orbit
- Ω_S Angle in the ecliptic between the point of Aries and the direction to the Sun (right ascension of the Sun)
- δ_S Declination of the Sun. $\sin\delta_S = \sin\phi \cdot \sin\Omega_S$ for circular planetary orbits
- ϕ Inclination of planet's equatorial plane relative to the ecliptic. $\phi = 23.44°$ for Earth

U. Walter, *Astronautics*, https://doi.org/10.1007/978-3-319-74373-8_14

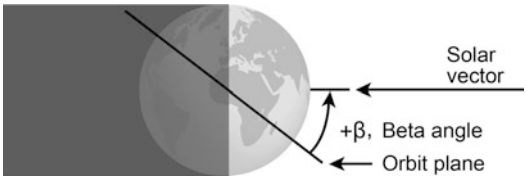

Fig. 14.1 The beta angle β is the angle between the solar vector and the orbit plane

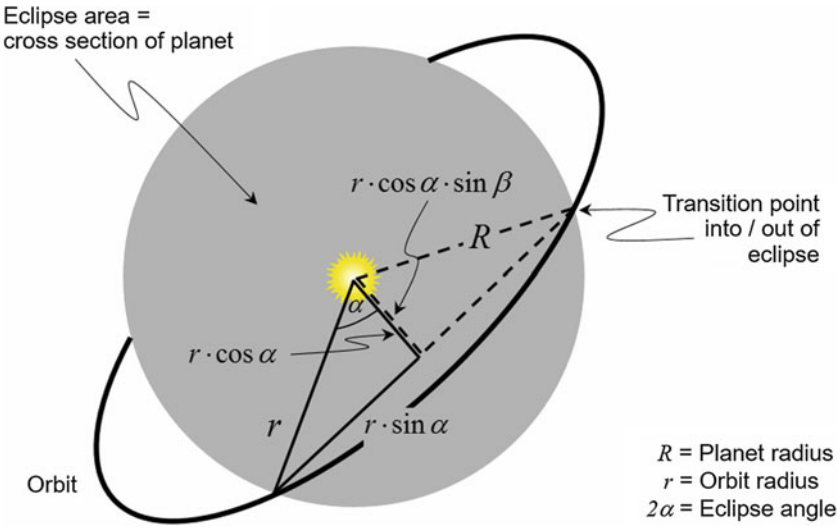

Fig. 14.2 Geometry of a circular orbit with radius r about a spherical planet with radius R and its path through the eclipse. Because the view is through the planet's center towards the Sun, the gray area is the dark side of the planet. The bold triangle with eclipse half angle α lies in the orbit plane, while the dashed triangle is its projection onto the plane perpendicular to the direction of view

Observe that Ω is a rapid variable relative to δ_S (see Sect. 12.3.3). Therefore $-1 \leq \sin(\Omega - \Omega_S) \leq 1$ and hence the beta angle varies for one RAAN revolution between

$$i - \phi \leq i - \delta_S \leq \beta \leq i + \delta_S \leq i + \phi \tag{14.1.2}$$

We now consider an arbitrary circular orbit with orbit radius r about a spherical planet with radius R. Figure 14.2 displays the orbit and eclipse geometry as viewed through the planet's center towards the Sun.

If we denote t_E to be the eclipse duration and 2α the eclipse angle, then

$$t_E = \frac{2\alpha}{360^\circ} T$$

where T is the orbital period. To determine the eclipse duration, we have to derive the eclipse angle. From Fig. 14.2 we find

$$R^2 = r^2 \cos^2\alpha \cdot \sin^2\beta + r^2 \sin^2\alpha = r^2\left(\sin^2\alpha \cdot \cos^2\beta + \sin^2\beta\right)$$

where α is half the eclipse angle and the latter expression follows after some trigonometrical expansions. Solving for α yields

$$\sin\alpha = \frac{\sqrt{(R/r)^2 - \sin^2\beta}}{\cos\beta} =: \frac{\sqrt{\sin^2\beta_* - \sin^2\beta}}{\cos\beta}$$

Here we have defined the limiting angle β_*. Obviously, only for $\beta < \beta_* := \arcsin(R/r)$ is the radicand positive and an eclipse exists. So, the condition for an eclipse reads

$$\sin\beta \le \frac{R}{r} \quad \textbf{eclipse condition} \tag{14.1.3}$$

From the above equation we alternatively find

$$\cos\alpha = \frac{\sqrt{r^2 - R^2}}{r\cos\beta}$$

which finally yields for the eclipse duration

$$t_E = \frac{T}{180^\circ} \arccos\frac{\sqrt{r^2 - R^2}}{r\cos\beta} \quad \textbf{eclipse duration} \tag{14.1.4}$$

Example

What is the time of the year, when a geostationary satellite is in eclipse and what is the maximal eclipse duration?

A GEO satellite experiences maximal eclipse if the Sun, the center of Earth, and the satellite lie on a line. This happens twice a year, namely at the vernal and autumnal equinoxes (see Fig. 13.1), which are on March 21 and September 23. We then have $\beta = 0$ and hence

$$t_E = \frac{23.934\ h}{180^\circ} \arccos\frac{\sqrt{42166^2 - 6378.1^2}}{42166} = 69.4\,\text{min}$$

Because we treat the Sun as a point source, this is the time between the middle of the entry and exit penumbras. Because the penumbra in GEO lasts 6 min, the duration of the umbra is 63.4 min and the total eclipse time 75.4 min. The condition for eclipse limit in GEO reads, with $i = 0$

$$\sin\beta = \sin 23.44^\circ \cdot \sin\Omega_S = R/r = 0.15126$$

Therefore, the days in eclipse are

$$\text{equinox} \pm \frac{365.2425\,\text{days}}{360^\circ} \arcsin\Omega_S = \text{equinox} \pm 22.7\,\text{days}$$

We finally determine those orbits that within a year and over several revolutions are steadily exposed to sunlight, i.e. do not suffer eclipse. This is the so-called *hot case* for a satellite (see Chap. 16, Problem 3). From Eqs. (14.1.2) and (14.1.3) it follows that this happens if

$$\max(\sin\beta) = \sin(i+\phi) > \frac{R}{r} \tag{14.1.5}$$

with $\phi = 23.44^\circ$ for Earth.

14.1.2 Access Area

The true outer horizon marks the theoretical limit of the observable area (access area) as seen from space, which ends at the horizon. The knowledge of the distance to the horizon is an important piece of information for Earth observation satellites, but also for astronauts in space. Even space travelers before a suborbital flight have asked me the question: How far can I see on Earth? The answer is given here.

For the sake of simplicity, we assume a spherical planet, which for practical purposes is quite a good approximation. Figure 14.3 depicts the geometry of a satellite above a planet.

Let R be the planetary radius and h the altitude of the satellite above the subsatellite point (nadir). Then for the rectangular triangle with the right angle at the true outer horizon, we have

$$\cos\lambda_0 = \frac{R}{R+h}$$

Let b_0 be the segment of a circle from the subsatellite point (a.k.a. nadir) to the horizon. Then

$$b_0 = \lambda_0 R = R \cdot \arccos\frac{R}{R+h} \quad \textbf{distance to true outer horizon} \tag{14.1.6}$$

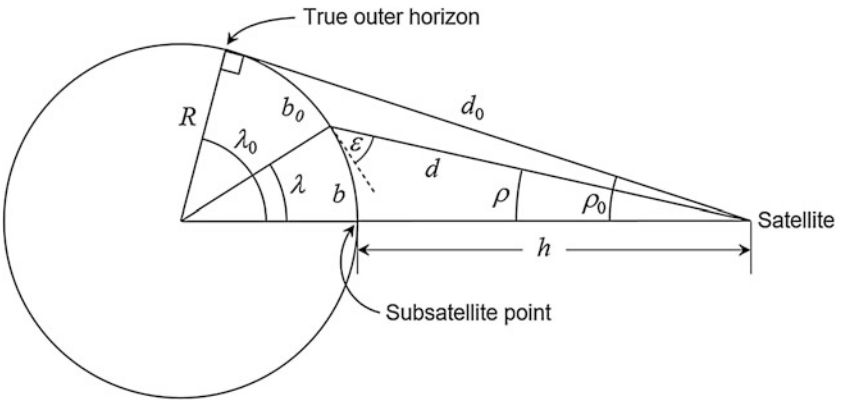

Fig. 14.3 Geometry of a satellite at altitude h above a planet's surface

For LEO satellites with $h \leq 1000\,\text{km} \ll R_\oplus$ we are looking for an approximation for b_0. From

$$\begin{aligned}\arccos\frac{R}{R+h} &= \arcsin\sqrt{1-\left(\frac{1}{1+h/R}\right)^2} \\ &= \sqrt{2\frac{h}{R}}\left[1-\frac{5}{12}\frac{h}{R}+\frac{42}{156}\left(\frac{h}{R}\right)^2+O\left(\frac{h^3}{R^3}\right)\right]\end{aligned}$$

we obtain the following approximations for LEOs

$$\begin{aligned} b_0 &\approx \sqrt{2hR_\oplus}\cdot\left(1-\tfrac{5}{12}\tfrac{h}{R_\oplus}\right) \quad @ \quad \text{error } < 1\% \\ &\approx \sqrt{2hR_\oplus} \qquad\qquad\quad @ \quad \text{error } = 6.5\%\cdot\tfrac{h}{1000\,\text{km}} \end{aligned} \qquad @\ \text{LEO} \qquad (14.1.7)$$

The so-called *instantaneous access area* (IAA) is the spherical segment (expressed in solid angle) of a planet as seen by a satellite at an instantaneous point on the orbit. With the above it is given as

$$\Omega_{IAA} = 2\pi(1-\cos\lambda_0) = 2\pi\frac{h}{R+h} \quad \textbf{instantaneous access area} \qquad (14.1.8)$$

Note that the actually observable part for Earth's surface might be much smaller due to atmospheric impairments such as fog or clouds, or twilight, etc.

Examples

These are the distances b_0 from nadir to Earth's horizon for some typical altitudes:

Eye level	$h = 1.7\,\text{m}$,	$b_0 = 4.7\,\text{km}$
Top of a house	$h = 10\,\text{m}$,	$b_0 = 11.3\,\text{km}$
Top of a hill	$h = 100\,\text{m}$,	$b_0 = 35.7\,\text{km}$
Top of a mountain	$h = 1000\,\text{m}$,	$b_0 = 113\,\text{km}$
Edge of space(suborbital flight)	$h = 100\,\text{km}$,	$b_0 = 1122\,\text{km}$
International Space Station:	$h = 350\,\text{km}$,	$b_0 = 2066\,\text{km}$

Suborbital space travelers should be aware of the fact that the horizon is too oblique to see anything there. Therefore, and for the above atmospheric reasons, at an altitude of 100 km surface details will be seen only for distances up to about 700 km.

14.2 Orbit Determination

This section deals with the problem of how to determine orbit elements, so that the path of a satellite is known and can be propagated (see Sects. 7.4.7 and 7.4.8 for orbit propagation). The most convenient way, surely, is to look them up in NORAD's two-line elements (TLE, see e.g. www.space-track.org). But sometimes they need to be determined faster or better, for instance, when a satellite has been launched into space and its orbit needs to be known immediately. So, how are the orbital elements of an actual orbit determined? This section is aimed at giving an answer to this question.

To be able to specifically determine the six orbital elements for a given S/C, we need to observe at least six suitable components of $\boldsymbol{r}$ or $\boldsymbol{v}$ of the S/C, which we call *orbital parameters*. As observables always include errors of observation, they also bring about errors of the derived orbital elements. So, to improve the accuracy of the derived orbital elements, far more than six observations are usually taken. Usually some orbit parameters are determined several times successively. Apart from observational errors, orbit perturbations occur due to gravitational asymmetries, solar winds, drag, etc. To determine the exact orbit under all these constraints, we need specific methods, which will be explained in the following.

14.2.1 Orbit Tracking

Orbit determination comes in two steps. First the satellite needs to be detected in its orbit by orbit tracking. The concept of tracking is considered in this sub-section. Thereafter the tracking data need to be converted by mathematical means into the orbital elements. Such methods will be presented in the remaining sub-sections.

Radar Tracking
Orbit tracking is usually done with ground-based parabolic radar antennas, which are directed toward the satellite in question (see Fig. 14.4). A signal is sent to the

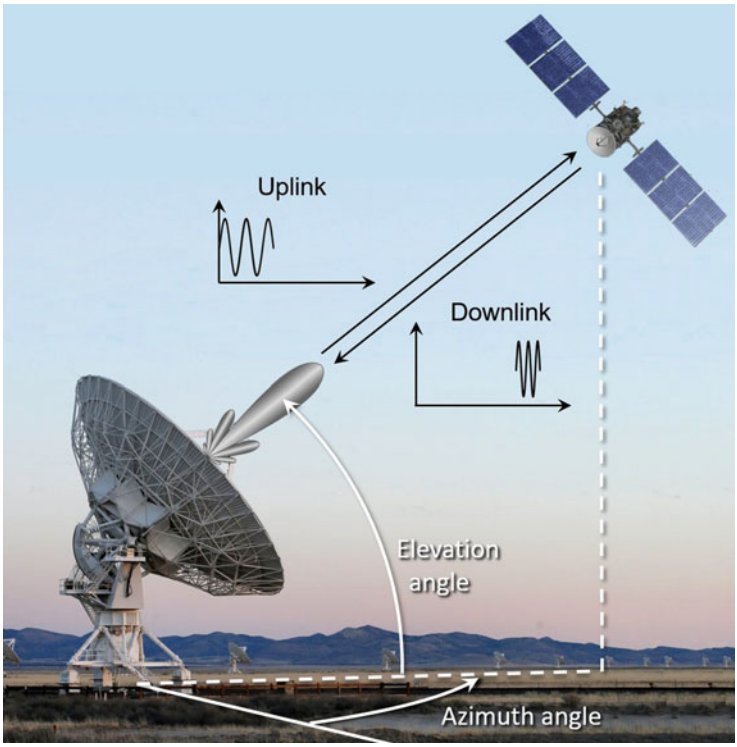

Fig. 14.4 Classical measurements of pointing angles, 2-way slant range, and Doppler shift to determine the range rate of a satellite

satellite and either a passively reflected signal is detected or a transponder on-board the satellite returns the signal with a well-known response time (Fig. 14.5). Either way, radar tracking provides us with the following orbital parameters:

- *Azimuth* and *elevation* (pointing angles) of the receiving antenna in the topocentric system of the ground station by tracking the direction of the maximum of the received signal. An antenna with the diameter of 15 m has an angle resolution of typically 0.1°.
- *Distance* (two-way ranging) from the ground station to the S/C by measuring the runtime of the returned signal with accuracy between 1 and 20 m.
- *Radial velocity* (range rate) with regard to the ground station by measuring the Doppler shift of the returned signal with an accuracy of $0.1-1\,\mathrm{mm\,s^{-1}}$.

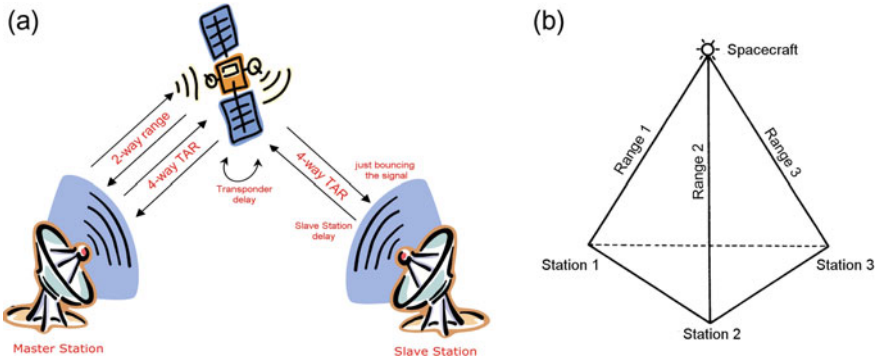

Fig. 14.5 **a** With 4-way TAR a signal from the master ground station is sent to the satellite, which redirects it to a slave station, which bounces the signal back to the satellite and back to the master ground station. **b** Having measured the ranges from at least three ground stations the exact orbit position can be determined by triangulation. *Credit* ESA

Turn-Around Ranging

In 2-way turn-around ranging (TAR) the satellite redirects the signal from a master ground station to a slave station, which by means of precise timing measures the runtime of the signal. The operational costs of such a (usually manned) slave station is quite high. Therefore 4-way TAR is often employed with an unmanned slave station that just bounces the signal back to the satellite, which redirects the signal back to the master ground station (Fig. 14.5a). From both, 2-way TAR and 4-way TAR, the ranges between the two stations and the satellite can be derived. By including two or more slave stations three or more different ranges can be determined. By triangulation this delivers the orbit position (Fig. 14.5b) with an accuracy of typically 2–3 m.

Deep Space Tracking

For deep space missions with many perturbation effects on the trajectory it is vital to know and hence to determine the position of the spacecraft regularly, in particular with high accuracy for fly-by maneuvers. NASA and ESA therefore augment the conventional ranging and doppler tracking by a the so-called ΔDOR (a.k.a. Delta-DOR, Delta-Differential One-Way Ranging) technique. The ΔDOR principle is simple (see Fig. 14.6). The deep space spacecraft transmits a signal, which is received by two ground stations, having a baseline as large as possible, with a certain delay time due to the slightly different distances to the ground stations. However, the delay time is affected by some sources of error: The radio waves travelling through the troposphere, ionosphere and solar plasma are diffracted differently. These errors are corrected by ΔDOR by tracking a quasar—an active galatic nucleus—that is seen in a direction close to the spacecraft (less than 10°) for calibration. Quasar positions are known extremely accurately through astronomical measurements, typically to a couple of nanoradians. The delay time of the quasar is subtracted from that of the spacecraft to provide the ΔDOR measurement.

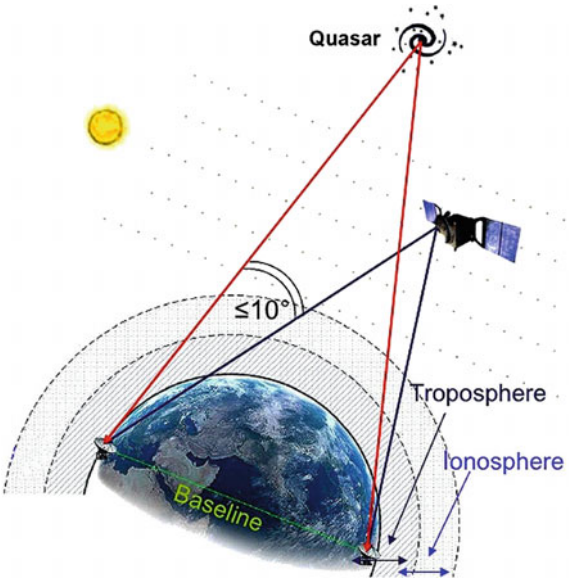

Fig. 14.6 The ΔDOR measuring principle. *Credit* ESA

To provide the full information of the spacecraft's position, two ΔDOR measurements at two baselines involving at least three groundstations are performed. This determines the accurate direction, which together with the classical ranging measurement determines the accurate position.

Other Tracking Systems

Tracking from ground stations has the disadvantage that the satellite can be observed only during the short time of overpass, so it is relatively inaccurate. NASA solved this problem by taking orbital data with its *Tracking and Data Relay Satellites* (TDRS) in GEO. Currently nine satellites are in use clustered near 41°W and 171°W and one satellite at 275°W. So they are separated from each other by 130° longitude and centered around White Sands Ground Terminal in New Mexico. However only two are active at the same time. Thus they cover 85–100% of all LEO satellites.

Today optical tracking systems, such as the Satellite Laser Ranging of the US Natural Environment Research Council (NERC) (see Fig. 14.7), or imaging systems, such as the US Ground-based Electro-Optical Deep Space Surveillance Telescope (GEODSS), are also used. Imaging systems reach an angle resolution of typically one arcsecond, and thus are far more accurate than radars. Laser ranging systems also have a better angle resolution and have the additional advantage that they do not require a satellite transponder. On the other hand, they do not work when it is cloudy. They determine the range from the runtime of a signal reflected from the satellite's surface quite accurately to just about 1 cm.

All ground-based systems suffer from the refraction (changes of the ray's path due to varying atmospheric density) of signals by the atmosphere (atmospheric

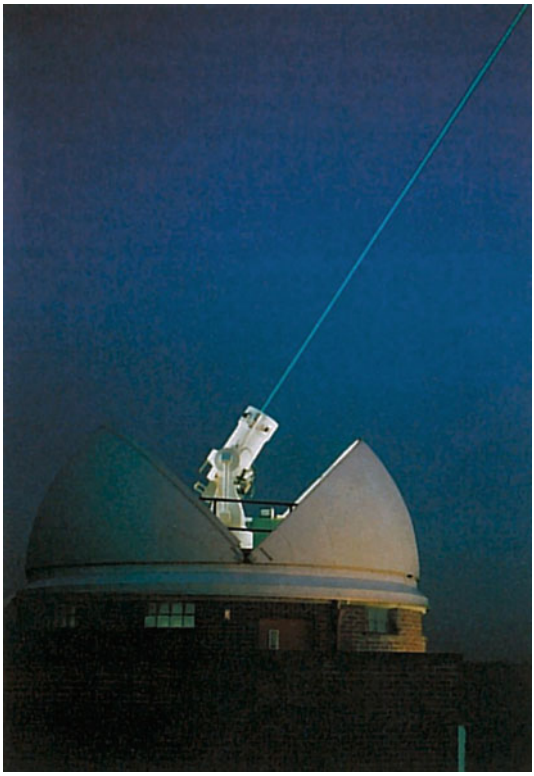

Fig. 14.7 Satellite laser ranging at NERC. *Credit* Montenbruck (2000)

refraction and ionospheric refraction), which moreover is time-dependent. If the orbits are to be tracked accurately, these effects have to be accounted for, which is a quite complex task. So, the complexity of tracking a satellite increases with the required accuracy. This general rule seems to have been turned upside down lately by the advent of space-qualified GPS receivers on-board a spacecraft. These receivers not only are relatively cheap, but also allow position and velocity determination on-board the S/C in real time. The advantage here is that orbit determination and possible required orbit corrections can be determined onboard. Orbit determination efforts are thus transferred from the ground station to the spacecraft, which considerably reduces mission control efforts on ground.

14.2.2 Generalized Orbit Determination Method

In the following, we first expound a general orbit determination method to determine the orbital elements independent of the type of measurements (position vectors, and/

or angles-only measurements, and/or radial velocity measurements, all those with or without time stamps). Section 14.2.3 will give an example for GEO determination. Only thereafter, will we outline three other established simple and elegant methods in Sects. 14.2.4, 14.2.5, and 14.2.6.

Overall, the orbit determination (measurement model) approach comprises two steps: Determination of the

1. orientation of the orbital plane, i.e. determine i, Ω,
2. shape of the orbit and orbit alignment, i.e. the metric elements a, e and the argument of periapsis ω, respectively.

The first step is straightforward and actually requires only the measurement of two sets of tracking data angles. The second step is the difficult part of the problem, which will be generalized.

Orientation of the Orbital Plane

Suppose we have two (= minimum requirement) point angles (i.e. angles-only) measurements or more in time sequence

$$\hat{\boldsymbol{r}}_1, \ldots, \hat{\boldsymbol{r}}_n, \; n \geq 2 \quad \text{pointing angles}$$

measured in a reference frame, which generally is the Cartesian equatorial coordinate system IJK of a planet having coordinate axes with unit vectors $\boldsymbol{u}_I$, $\boldsymbol{u}_J$, $\boldsymbol{u}_K$. From $\hat{\boldsymbol{r}}_1, \ldots, \hat{\boldsymbol{r}}_n$ we choose two vectors $\hat{\boldsymbol{r}}_i$, $\hat{\boldsymbol{r}}_j$, from which the angular momentum unit vector

$$\hat{\boldsymbol{h}} = \frac{\hat{\boldsymbol{r}}_i \times \hat{\boldsymbol{r}}_j}{\left|\hat{\boldsymbol{r}}_i \times \hat{\boldsymbol{r}}_j\right|}$$

is determined and with it the invariant orbital plane. Because $\hat{\boldsymbol{h}}$ is key to the following calculations, it is clear that owing to numerical stability reasons $\hat{\boldsymbol{r}}_i$, $\hat{\boldsymbol{r}}_j$ have to be chosen such that $\left|\hat{\boldsymbol{r}}_i \times \hat{\boldsymbol{r}}_j\right| = \sin \angle\left(\hat{\boldsymbol{r}}_i, \; \hat{\boldsymbol{r}}_j\right) = \max$, i.e. they should be perpendicular to each other as far as possible. This directly yields the inclination of the orbit

$$i = \arccos\left(\boldsymbol{u}_K \hat{\boldsymbol{h}}\right) \tag{14.2.1}$$

In addition, we have for the unit vector to the ascending node of the orbit

$$\boldsymbol{u}_n = \frac{1}{\sin i}\left(\boldsymbol{u}_K \times \hat{\boldsymbol{h}}\right) \quad \text{ascending node vector}$$

Therefore and because $\boldsymbol{u}_K(\boldsymbol{u}_I \times \boldsymbol{u}_n) = \boldsymbol{u}_J \boldsymbol{u}_n$ we have for RAAN

$$\Omega = \begin{cases} \arccos(\boldsymbol{u}_I \boldsymbol{u}_n) & @ \ \ \boldsymbol{u}_J \boldsymbol{u}_n \geq 0 \\ 2\pi - \arccos(\boldsymbol{u}_I \boldsymbol{u}_n) & @ \ \ \boldsymbol{u}_J \boldsymbol{u}_n < 0 \end{cases} \tag{14.2.2}$$

such that $0 \leq \Omega \leq 2\pi$. Needless to say that, by the same token as above, the node vector and with it RAAN becomes indeterminate with vanishing inclination. We further have per definition

$$\boldsymbol{u}_n \hat{\boldsymbol{r}}_i = \cos u_i \quad @ \ \ i = 1, \ldots, n$$

where

$$u = \theta + \omega \qquad \text{argument of latitude}$$

is the so-called *argument of latitude* (see Sect. 7.3.5) with $0 \leq u \leq 2\pi$, and θ, ω are the orbit angle and the argument of periapsis, respectively. Because $\hat{\boldsymbol{h}}(\boldsymbol{u}_n \times \hat{\boldsymbol{r}}_i) = \hat{\boldsymbol{r}}_i\left(\hat{\boldsymbol{h}} \times \boldsymbol{u}_n\right) = \hat{\boldsymbol{r}}_i\left[\hat{\boldsymbol{h}} \times \left(\boldsymbol{u}_K \times \hat{\boldsymbol{h}}\right)\right] = \boldsymbol{u}_K \hat{\boldsymbol{r}}_i$ we determine u_i from the pointing angles as

$$u_i = \begin{cases} \arccos(\boldsymbol{u}_n \hat{\boldsymbol{r}}_i) & @ \ \ \boldsymbol{u}_K \hat{\boldsymbol{r}}_i \geq 0 \\ 2\pi - \arccos(\boldsymbol{u}_n \hat{\boldsymbol{r}}_i) & @ \ \ \boldsymbol{u}_K \hat{\boldsymbol{r}}_i < 0 \end{cases} \tag{14.2.3}$$

In summary, the orientation of the orbital plane can be determined straight away from merely two angles-only measurements.

Orbit Shape and Orbit Alignment

We now come to the cornerstone of the generalization of orbit determination, namely to derive the other orbital elements from the tracking data. There may be a number of k measurements, which provide the radial vectors $\boldsymbol{r}_1, \ldots, \boldsymbol{r}_k$, i.e. in addition to the angles also the orbit radii. In this case, the following orbit equations must apply

$$r_i = \frac{a(1 - e^2)}{1 + e \cos \theta_i} \quad @ \ \ i = 1, \ldots, k$$

Applying $\theta_i = u_i - \omega$, we derive from these the f-functions

$$f_i = 1 + e \cos(u_i - \omega) - \frac{a(1 - e^2)}{r_i} \quad @ \ \ i = 1, \ldots, k \tag{14.2.4}$$

The rationale of the f-functions is, only if we find the right orbital elements that fit the measured data, then $f_i = 0$.

Some measurements may also come with time stamps $t_1, \ldots, t_l$. For those Kepler's equation must apply

$$n \cdot \left(t_i - t_p\right) = E_i - e \, \sin E_i \quad @ \quad i = 1, \ldots, l$$

where $n = \sqrt{\mu/a^3}$ and t_p is the unknown epoch, i.e. the time at passage through the periapsis. To apply the measured μ_i we make use of Eq. (7.4.14b)

$$\sin E_i = \frac{\sqrt{1-e^2}\,\sin(u_i - \omega)}{1 + e\,\cos(u_i - \omega)}$$

and insert it into Kepler's equation, which we rewrite as

$$\sin E_i = \sin\left[n \cdot \left(t_i - t_p\right) + e \, \sin E_i\right]$$

This gives rise to the g-functions

$$g_i = \sin\left[\sqrt{\frac{\mu}{a^3}}\cdot\left(t_i - t_p\right) + e\frac{\sqrt{1-e^2}\,\sin(u_i - \omega)}{1 + e\,\cos(u_i - \omega)}\right] - \frac{\sqrt{1-e^2}\,\sin(u_i - \omega)}{1 + e\,\cos(u_i - \omega)} \quad @ \quad i = 1, \ldots, l \qquad (14.2.5)$$

serving the same purpose as the f-functions.

Finally, there may be a number of m radial velocity (range rate) measurements $\dot{r}_i$. From Eq. (7.3.15a) we directly obtain the according h-functions

$$h_i = \dot{r}_i - e\sqrt{\frac{\mu}{a(1-e^2)}}\,\sin(u_i - \omega) \quad @ \quad i = 1, \ldots, m$$

Now that we have developed the body of our generalized method, we are flexible enough to accept any type of measurement to derive the wanted quantities a, e, ω from the roots of the applying functions f_i, g_i, h_i. Here we list some typical cases: Given

- 3 measurements of the position vector: $\boldsymbol{r}_1, \boldsymbol{r}_2, \boldsymbol{r}_3$.
  $\rightarrow f_1 = f_2 = f_3 = 0$. From these three equations a, e, ω can derived.
- 2 measurements of the position vector and their time stamps: $\boldsymbol{r}_1, \boldsymbol{r}_2 |\ t_1, t_2$.
  $\rightarrow f_1 = f_2 = g_1 = g_2 = 0$. From these four equations a, e, ω, t_p can derived.
- 4 measurements of pointing angles and their time stamps: $\hat{\boldsymbol{r}}_1, \hat{\boldsymbol{r}}_2, \hat{\boldsymbol{r}}_3, \hat{\boldsymbol{r}}_4 |\ t_1, t_3, t_3, t_4$. This is the re-known and so-called *angles-only orbit determination*.
  $\rightarrow g_1 = g_2 = g_3 = g_4 = 0$. From these four equations a, e, ω, t_p can derived.
- 2 position vectors plus their range rates.
  $\rightarrow f_1 = f_2 = h_1 = h_2 = 0$. From these four equations a, e, ω can be derived.

The method of choice to find the root of n variables from n nonlinear f, g, and h functions is Newton's method for n dimension, plus applying unitary Householder transformations for solving the set of linear equations $\boldsymbol{A}_{3\times 3}\boldsymbol{x} = \boldsymbol{b}$ in the first case, as part of the method, and $\boldsymbol{A}_{4\times 4}\boldsymbol{x} = \boldsymbol{b}$ in the second and third case. Unitary Householder transformations have the unique property that they do not degrade the numerical condition of the problem if, for instance the variables exhibit different orders of magnitude.

Finally, let us assume that we have more f, g, and h functions than the 4 variables a, e, ω, t_p

$$\begin{array}{l} f_1, \ldots, f_k = 0 \\ g_1, \ldots, g_l = 0 \\ h_1, \ldots, h_m = 0 \end{array} \qquad @ \quad k + l + m > 4$$

which is the case for instance when there are a great many measurements. To solve such an over-determined system is called the *least squares problem*. The prefered way for solving for a, e, ω, t_p is also by Newton's method, this time by a 4-dimensional type and again applying unitary Householder transformations to $\boldsymbol{A}_{4\times(k+l)}\boldsymbol{x} = \boldsymbol{b}$. The unitarity of the Householder transformations is here particularly useful if the overdetermined set of equations comes along with some ill-conditioned measurements.

14.2.3 GEO Orbit from Angles-Only Data

As a sample application of the generalized orbit determination method, suppose the orbital elements of a GEO satellite need to be determined by angles-only measurements with time stamps. As a first step the elements i, Ω and the quantities u_i are derived as described in the above generalized orbit determination method. The specific property of a GEO orbit is that

$$a_{GEO} = 42\,166.26\,\text{km}$$

is well-known and hence $n = \sqrt{\mu/a_{GEO}^3} = 1/(3.80957\,\text{h})$, and that $e \ll 1$. Owing to the latter peculiarity we can simplify the g-functions. To do so, we revert to Eq. (7.4.19c) from which follows

$$\theta = u - \omega \approx M + 2e\,\sin M \tag{14.2.6}$$

We apply this key equation to the measurement differences $\Delta\theta_{ji} = \theta_j - \theta_i$, $\Delta u_{ji} = u_j - u_i$, $\Delta t_{ji} = t_j - t_i$, and

$$M_k := n(t_k - t_p) =: nt_k - \tau_p$$

We thus get

$$\begin{aligned} \Delta u_{21} &\approx \Delta t_{21} + 2e[\sin M_2 - \sin M_1] \\ \Delta u_{32} &\approx \Delta t_{32} + 2e[\sin M_3 - \sin M_2] \end{aligned}$$

$$\rightarrow \quad \begin{aligned} 2e[\sin M_2 - \sin M_1] &\approx \Delta u_{21} - n \cdot \Delta t_{21} \\ 2e[\sin M_3 - \sin M_2] &\approx \Delta u_{32} - n \cdot \Delta t_{32} \end{aligned}$$

Now we eliminate the eccentricity by deviding both equations

$$\frac{\sin M_2 - \sin M_1}{\sin M_3 - \sin M_2} \approx \frac{\Delta u_{21} - n \cdot \Delta t_{21}}{\Delta u_{32} - n \cdot \Delta t_{32}}$$

which yields the wanted g-function

$$g(\tau_p) = (\Delta u_{32} - n \cdot \Delta t_{32})[\sin M_2 - \sin M_1] - (\Delta u_{21} - n \cdot \Delta t_{21})[\sin M_3 - \sin M_2]$$

The Newton-iteration $\tilde{\tau}_p = \tau_p - f(\tau_p)/f'(\tau_p)$ to derive τ_p as the root of $g(\tau_p)$ reads in our case

$$\tilde{\tau}_p = \tau_p + \frac{(\Delta u_{32} - n \cdot \Delta t_{32})[\sin M_2 - \sin M_1] - (\Delta u_{21} - n \cdot \Delta t_{21})[\sin M_3 - \sin M_2]}{(\Delta u_{32} - n \cdot \Delta t_{32})[\cos M_2 - \cos M_1] - (\Delta u_{21} - n \cdot \Delta t_{21})[\cos M_3 - \cos M_2]}$$

where $M_i = nt_i - \tau_p$. With the iterative solution $\tau_p = nt_p$ and from the above equations, modified for better numerical stability, the eccentricity is obtained as

$$e = \frac{1}{2} \frac{\Delta u_{31} - n \cdot \Delta t_{31}}{\sin M_3 - \sin M_1} \tag{14.2.7}$$

Finally, Eq. (14.2.6) yields for any measurement i

$$\omega = u_i - M_i - 2e \sin M_i \tag{14.2.8}$$

In conclusion, we see that for GEO orbit determination only 3 pointing angles, plus corresponding time stamps are needed. This is one less measurement than in the general case because a is known a priori.

The determination of GEO elements becomes even simpler if the satellite motion in the guiding center system is constantly recorded as shown in Fig. 12.28. Then, according to Sect. 12.5.3, subsection *East–West Station-Keeping Strategies*, the inclination and eccentricity of a GEO can be read directly from the record: The North-South motion

width of one daily cycle is twice the inclination and the width of the East-West motion width equals $4e$. With the eccentricity e thus derived, there is only ω left to be determined. For that we recall Eq. (14.2.6) and make use of the fact that for the first order term $M \approx \theta = u - \omega$ holds. Hence

$$n(t - t_p) = (u - \omega) - 2e \sin(u - \omega)$$

From two point angles u_1, u_2 with time stamps t_1, t_2 and by taking differences of two equations, thus eliminating t_0, we get

$$n \cdot \Delta t_{21} = \Delta u_{21} - 2e[\sin(u_2 - \omega) - \sin(u_1 - \omega)]$$

By applying the trigonometric relation

$$\sin(u_2 - \omega) - \sin(u_1 - \omega) = 2 \sin \frac{\Delta u_{21}}{2} \cos \frac{u_1 + u_2 - 2\omega}{2}$$

we can solve for ω and finally get

$$\omega = \frac{1}{2}\left\{u_1 + u_2 - 2 \arccos\left[\frac{\Delta u_{21} - n \cdot \Delta t_{21}}{4e \sin(\Delta u_{21}/2)}\right]\right\}$$

14.2.4 Simple Orbit Estimation

For a preliminary estimation of the state vector, the following method is suitable. It is based on the position vectors $\boldsymbol{r}_0, \boldsymbol{r}_+$ measured at the small time interval Δt, typically in the course of a LEO satellite pass. From Eqs. (14.2.1) and (14.2.2) we immediately derive i, Ω.

Now, let $\boldsymbol{r}_0 := \boldsymbol{r}(0)$ be the position vector at the first observation time $t_0 = 0$. Any time later it can be expressed as a Taylor series

$$\boldsymbol{r} \approx \boldsymbol{r}_0 + \dot{\boldsymbol{r}}_0 t + \frac{1}{2}\ddot{\boldsymbol{r}}_0 t^2 + \frac{1}{6}\dddot{\boldsymbol{r}}_0 t^3 \tag{14.2.9}$$

From this follows by differentiation that

$$\ddot{\boldsymbol{r}} = \ddot{\boldsymbol{r}}_0 + \dddot{\boldsymbol{r}}_0 t \tag{14.2.10}$$

We now apply Newton's equation of motion $\ddot{\boldsymbol{r}} = -\gamma \boldsymbol{r}$ with $\gamma := \mu/r^3$

$$-\gamma \boldsymbol{r} = \ddot{\boldsymbol{r}}_0 + \dddot{\boldsymbol{r}}_0 t$$

from which with Eq. (14.2.10) and with the definition $\boldsymbol{r}_+ := \boldsymbol{r}(t_+) = \boldsymbol{r}(t_0 + \Delta t) = \boldsymbol{r}(\Delta t)$ it follows that

$$-\gamma_0 \boldsymbol{r}_0 = \ddot{\boldsymbol{r}}_0$$
$$-\gamma_1 \boldsymbol{r}_+ = \ddot{\boldsymbol{r}}_0 + \dddot{\boldsymbol{r}}_0 \cdot \Delta t$$

Solving these equations for $\ddot{\boldsymbol{r}}_0$ and $\dddot{\boldsymbol{r}}_0$ and inserting the results into Eq. (14.2.9) for $\boldsymbol{r}_+ = \boldsymbol{r}(\Delta t)$ one obtains for $\dot{\boldsymbol{r}}_0 \equiv \boldsymbol{v}_0$

$$\boldsymbol{v}_0 = \frac{\boldsymbol{r}_+ - \boldsymbol{r}_0}{\Delta t} + \frac{\mu}{6}\left(\frac{2\boldsymbol{r}_0}{r_0^3} + \frac{\boldsymbol{r}_+}{r_+^3}\right) \cdot \Delta t \tag{14.2.11}$$

If three subsequent measurements $\boldsymbol{r}_-(t_-), \boldsymbol{r}_0(t_0), \boldsymbol{r}_+(t_+)$ are taken at small time intervals, then it can be shown (Herrick and Gibbs) and $\Delta t_{ij} = t_i - t_j > 0$ that

$$\begin{aligned}\boldsymbol{v}_0 = {} & \Delta t_{+0}\left[\frac{\mu}{12r_-^3} - \frac{1}{\Delta t_{0-}\Delta t_{+-}}\right]\boldsymbol{r}_- + (\Delta t_{+0} - \Delta t_{0-})\left[\frac{\mu}{12r_0^3} + \frac{1}{\Delta t_{0-}\Delta t_{+0}}\right]\boldsymbol{r}_0 \\ & + \Delta t_{0-}\left[\frac{\mu}{12r_+^3} + \frac{1}{\Delta t_{+-}\Delta t_{+0}}\right]\boldsymbol{r}_+\end{aligned}$$

Thus the state vector $(\boldsymbol{r}_0, \boldsymbol{v}_0)$ is determined at time t_0. This so-called *Herrick-Gibbs method* works best for small geocentric angles, typically less than 15° for LEO and less than 6° for GSO, i.e. for successive measurements from one groundstation.

If the geocentric angles of the three subsequent measurements $\boldsymbol{r}_-, \boldsymbol{r}_0, \boldsymbol{r}_+$ are more appart than 15° for LEO and 6° for GSO, then the following *Gibbs method* is preferable

$$\begin{aligned}\boldsymbol{N} &:= r_-(\boldsymbol{r}_0 \times \boldsymbol{r}_+) + r_0(\boldsymbol{r}_+ \times \boldsymbol{r}_-) + r_+(\boldsymbol{r}_- \times \boldsymbol{r}_0) \\ \boldsymbol{D} &:= \boldsymbol{r}_0 \times \boldsymbol{r}_+ + \boldsymbol{r}_+ \times \boldsymbol{r}_- + \boldsymbol{r}_- \times \boldsymbol{r}_0 \\ \boldsymbol{S} &:= \boldsymbol{r}_-(r_0 - r_+) + \boldsymbol{r}_0(r_+ - r_-) + \boldsymbol{r}_+(r_- - r_0) \\ \boldsymbol{v}_0 &= \sqrt{\frac{\mu}{ND}}\left(\frac{\boldsymbol{D} \times \boldsymbol{r}_0}{r_0}\right) + \boldsymbol{S}\end{aligned}$$

As shown in Subsection *Conversion: State Vector → Orbital Elements* in Sect. 7.3.5 the orbital elements can easily obtained from these state vectors.

14.2.5 Modified Battin's Method

We present here an elegant method essentially described by Battin in his book *Astronautical Guidance* (Battin 1964, p. 22f) to determine the orbital elements directly from the measurements of three successive orbit radii r_1, r_2, r_3 and the angles between them $\Delta\theta_{ji} = \theta_j - \theta_i$. From the orbit equation we have

$$r_i = \frac{p}{1 + e\,\cos\theta_i} \quad @\ \ i = 1,\ 2,\ 3 \tag{14.2.12}$$

from which follows

$$e\,\cos\theta_i = \frac{p}{r_i} - 1 \qquad @\ \ i = 1,\ 2,\ 3 \tag{14.2.13}$$

$$e\,\sin\theta_i = \frac{r_j(p - r_i)\cos\Delta\theta_{ji} - r_i\big(p - r_j\big)}{r_{ji} r_j \sin\Delta\theta_{ji}} \quad @\ \ j \neq i \tag{14.2.14}$$

with

$$\Delta\theta_{ji} = \theta_j - \theta_i$$

Obviously, from any two position vectors one can derive p and e from Eq. (14.2.12). However, we seek for a numerically more stable solution where all three position vectors equally contribute, and which, in addition, merely makes use of intermediate angles. We therefore pick in Eq. (14.2.14) any position vector i, equate the two equations for $j \neq i$, and solve it for p. We thus get

$$p = \frac{r_1 r_2 r_3(\sin\Delta\theta_{23} + \sin\Delta\theta_{31} + \sin\Delta\theta_{12})}{r_2 r_3 \sin\Delta\theta_{23} + r_1 r_3 \sin\Delta\theta_{31} + r_1 r_2 \sin\Delta\theta_{12}} = a\big(1 - e^2\big) \tag{14.2.7}$$

To determine e, rather than making use of Eq. (14.2.13) as Battin does, we seek an equation for e, in which again only intermediate angles are required. We therefore make use of Eqs. (14.2.13) and (14.2.14) and for numerical stability choose those two vectors $\boldsymbol{r}_k$, $\boldsymbol{r}_l$, with property $\sin\angle\big(\boldsymbol{r}_i,\ \boldsymbol{r}_j\big) = \max$, i.e. they should be perpendicular to each other as much as possible. We thus determine $e^2 \sin\Delta\theta_{lk} = (e\,\sin\theta_l)(e\,\cos\theta_k) - (e\,\cos\theta_l)(e\,\sin\theta_k)$. From this follows

$$e^2 \sin\Delta\theta_{lk} = \left(\frac{p}{r_k} - 1\right)^2 + \left(\frac{p}{r_l} - 1\right)^2 - 2\left(\frac{p}{r_k} - 1\right)\left(\frac{p}{r_l} - 1\right)\cos\Delta\theta_{lk} \tag{14.2.15}$$

Thus, from Eqs. (14.2.7) and (14.2.15) the metric elements p, e, a can be determined.

To determine the orientation of the orbit, we make use of the fact that the eccentricity vector lies in the orbit plane spanned by the two position vectors $\boldsymbol{r}_k$, $\boldsymbol{r}_l$ with the said optimal property. Therefore

$$\boldsymbol{e} = \alpha\,\hat{\boldsymbol{r}}_k + \beta\,\hat{\boldsymbol{r}}_l$$

From this follows

$$\boldsymbol{er}_k = \alpha\, r_k + \beta\, r_k \cos\Delta\theta_{lk}$$
$$\boldsymbol{er}_l = \alpha\, r_l \cos\Delta\theta_{lk} + \beta\, r_l$$

Equating these equations with the two results from the orbit equation

$$\boldsymbol{er}_k = er_k \cos\theta_{ki} = p - r_k$$
$$\boldsymbol{er}_l = er_l \cos\theta_l = p - r_l$$

finally delivers

$$\begin{aligned}\alpha \sin^2\Delta\theta_{lk} &= \left(\frac{p}{r_k} - 1\right) - \left(\frac{p}{r_l} - 1\right)\cos\Delta\theta_{lk}\\ \beta \sin^2\Delta\theta_{lk} &= \left(\frac{p}{r_l} - 1\right) - \left(\frac{p}{r_k} - 1\right)\cos\Delta\theta_{lk}\end{aligned} \tag{14.2.16}$$

from which the wanted α, β can be extracted. Observe that this method is numerically stable for any conic orbit, even for $|a| \to \infty$. However, if the eccentricity is small, the direction of the eccentricity vector is not well established.

14.2.6 Advanced Orbit Determination

Considering Oblateness Perturbations

The methods expounded so far in Sect. 14.2 are based on the concept of the ideal 2-body problem, which is a fair approximation for just one orbit. However, any external force such as gravitational perturbations, lunisolar perturbations, or drag change the orbit over many revolutions, so that derived orbit elements apply only for the instantaneous osculating orbit (see Sect. 12.1.2). This implies that tracking data need to be taken over just one orbit. Even in the course of one orbit a low Earth orbit changes orientation slightly. As shown in Sect. 12.3.3 the oblateness perturbation induced changes $\dot\omega, \dot\Omega, \dot M$ in LEO are of order $10(R_\oplus/a)^{7/2}\left[^\circ\,\mathrm{day}^{-1}\right] \approx 0.5^\circ$ per orbit. Since tracking data have an angular resolution of typically 0.1°, oblateness perturbation matters in particular when tracking data are taken over more than one orbit.

A first remedy for LEO orbits that do not suffer under too great drag is to take the oblateness perturbations into account. According to Sect. 12.3.3 RAAN change between two data takes i, j with $t_j > t_i$ is

$$\Delta\Omega_{ji} = \Omega_j - \Omega_i = -n \cdot \Delta t_{ji} \cdot j_2 \cos i$$

with

$$j_2 = \frac{3}{2} J_2 \left[\frac{R_\oplus}{a(1-e^2)}\right]^2, \quad J_2 = 1.0826266 \times 10^{-3}$$

Therefore, of the two vectors $\hat{\boldsymbol{r}}_i$, $\hat{\boldsymbol{r}}_j$ with $t_j > t_i$, from which the angular momentum unit vector is determined, $\hat{\boldsymbol{r}}_j$ needs to be rotated back about the $\boldsymbol{u}_K$-axis by the RAAN change angle according to

$$\hat{\boldsymbol{r}}'_j = \begin{pmatrix} \cos(-\Delta\Omega_{ji}) & \sin(-\Delta\Omega_{ji}) & 0 \\ -\sin(-\Delta\Omega_{ji}) & \cos(-\Delta\Omega_{ji}) & 0 \\ 0 & 0 & 1 \end{pmatrix} \hat{\boldsymbol{r}}_j = \begin{pmatrix} \cos\Delta\Omega_{ji} & -\sin\Delta\Omega_{ji} & 0 \\ \sin\Delta\Omega_{ji} & \cos\Delta\Omega_{ji} & 0 \\ 0 & 0 & 1 \end{pmatrix} \hat{\boldsymbol{r}}_j$$

The rest of the generalized orbit determination procedure in Sect. 14.2.2 remains the same, namely

$$\hat{\boldsymbol{h}} = \frac{\hat{\boldsymbol{r}}_i \times \hat{\boldsymbol{r}}'_j}{\left|\hat{\boldsymbol{r}}_i \times \hat{\boldsymbol{r}}'_j\right|}, \quad \boldsymbol{u}_n = \frac{1}{\sin i}\left(\boldsymbol{u}_K \times \hat{\boldsymbol{h}}\right)$$

and

$$\Omega_i = \begin{cases} \arccos(\boldsymbol{u}_I \boldsymbol{u}_n) & @ \ \boldsymbol{u}_J \boldsymbol{u}_n \geq 0 \\ 2\pi - \arccos(\boldsymbol{u}_I \boldsymbol{u}_n) & @ \ \boldsymbol{u}_J \boldsymbol{u}_n < 0 \end{cases}$$

which now is the RAAN at the first data take i. Note that owing to $j_2 \cdot n \cdot \Delta t \ll 1$ for j_2 only an approximate value of a needs to be known. We recall that the inclination is not subject to change under oblateness perturbations.

According to the results at the end of Sect. 12.3.3 the expressions $u_i - \omega$, $\Delta\theta$, $(t_i - t_0)$ and Δt in all key equations (in particular in the f-functions, g-functions, and h-functions) in Sects. 14.2.2, 14.2.3 and 14.2.5 need to be substituted by

$$\begin{aligned} n(t_i - t_0) \quad &\rightarrow \quad \left[1 + j_2\left(1 - \tfrac{3}{2}\sin^2 i\right)\right] \cdot n(t_i - t_0) \\ n \cdot \Delta t \quad &\rightarrow \quad \left[1 + j_2\left(1 - \tfrac{3}{2}\sin^2 i\right)\right] n \cdot \Delta t \end{aligned}$$

$$\begin{aligned} u_i - \omega \quad &\rightarrow \quad u_i - \omega_k - 2j_2\left(1 - \tfrac{5}{4}\sin^2 i\right) \cdot n(t_i - t_k) \approx u_i - \omega_k - 2j_2\left(1 - \tfrac{5}{4}\sin^2 i\right) \cdot \Delta\theta_{ik} \\ \Delta\theta_{ik} \quad &\rightarrow \quad \Delta\theta_{ik} \cdot \left[1 + 2j_2\left(1 - \tfrac{5}{4}\sin^2 i\right)\right] \end{aligned}$$

This improved calculation determines the orientation of the apse line, ω_k, at the time where data with index k were taken.

Proficient Orbit Determination

A procedure that proficiently derives the orbital elements takes all orbit perturbations into account by solving the the 3-D equation of motion at each time a data take is taken, p for instance by Cowell's Method by Recurrence Iteration (see Sect. 12.2.4).

The solution then provides the time-dependent state vector, $(\boldsymbol{r}(t), \boldsymbol{v}(t))$, representing a comprehensive description of the orbit. The solution of the orbit tracking problem therefore is as follows:

1. Carry out a sufficient number of measurements of orbital parameters.
2. Use these tracking data to determine with a least-square method (for batch operation on ground) or Kalman filtering method (for on-board sequential real-time processing) the position and velocity of the S/C (so-called *orbit estimation*). This generates the so-called *measurement model* $(\boldsymbol{r}, \boldsymbol{v})_m$ of the state vector.
3. Use this measurement model as initial values to solve with numerical methods the equations of motion (see Sect. 12.2.4), the precision of which is chosen corresponding to the accuracy of the measurement model. The solution propagates the orbital state into the future and is called the *theoretical trajectory model* of the state vector $(\boldsymbol{r}, \boldsymbol{v})_t$.
4. Compare the predictions of the theoretical trajectory model with the measurement model updated by further measurements. To minimize the deviations of the two models–the so-called *residuals*—vary still unknown model parameters (such as drag coefficient or remaining atmospheric density). By this procedure, the still unknown model parameters are determined.
5. When propagation limits are reached, noticeable by increasingly unresolved residuals, a new iteration starts. The measurement model is updated by measurements (the so-called d*ifferential correction*). It is then used as updated initial values for the solver of the equations of motion, whereby the theoretical prediction of the orbit is improved.

This procedure clearly shows that this orbit determination method does not only accurately determine the trajectory, but that by adjusting the parameters of unknown perturbations one can also determine their characteristics. This is exactly the way by which the coefficients of the terrestrial potential (see Sect. 12.2.2) were determined with missions in the past, such as CHAMP, GRACE, or GOCE by high precision measurements of their orbits.

A detailed explication of how all these five steps are implemented, in practice, would be far beyond the scope of this book. For details, the interested reader should consult the books of Montenbruck and Gill (2000), Tapley et al. (2004), Vallado (2007), or Escobal (1965).